The effect of mean stress on the fatigue behaviour of woven-roving GFRP subjected to torsional moments

M.N. Abouelwafa, A. Gomaa, A. Hamdy, E. Morsi and M. Nasr
Mechanical Eng. Dept., Faculty of Eng., Alexandria University, Alexandria, Egypt

The effect of torsional mean stresses on the fatigue behaviour of Glass Fiber-Reinforced Polyester (GFRP) is studied via testing thin-walled, woven - roving specimens with two fibre orientations, [± 45°] and [0,90°], at negative stress ratios (*R*), *R* = -1, -0.75, -0.5, -0.25, 0. The [± 45°] $_{2s}$ specimens were found to have higher strength than the [0,90°] $_{2s}$ specimens, at all stress ratios; as being subjected to tension-compression local stress components, while the later being subjected to pure shear local stress. Under negative stress ratios; the mean stress component had a detrimental effect on the amplitude component for the [± 45°] $_{2s}$ specimens, while it was ineffective for the [0,90°] $_{2s}$ specimens for a certain region, then it had a detrimental effect the fatigue behaviour under positive stress ratios was studied theoretically. For the [± 45°] $_{2s}$ specimens, the expected positive stress ratio points failed to be related to the negative ones; while they show an acceptable behaviour for the [0,90°] $_{2s}$ specimens, tending to decrease the amplitude component for the same life.

تم دراسة تأثير وجود اجهادات التواء متوسطة على سلوك البوليستر المدعم بالياف زجاجية منسوجة (GFRP) شبكيا وذلك باختبار عينات اسطوانية رفيعة السمك يميل اتجاه الالياف فيها بالنسبة لمحور العينة فى اتجاهين (صفر، ٩٠°) و (± ٤٥°) . تمت هذه الدراسة عند نسب اجهادات سالبة ولقيم – ١ ، – ٠,٧٥ ، – ٠,٥ ، – ٠,٢٥ ، صفر. وقد وجد من هذه الدراسة أن العينات ذات الاتجاه (± ٤٥°) لها قدرة تحمل أعلى من العينات ذات (صفر ، ٩٠°) عند جميع نسب الاجهاد المختلفة و ذلك لان الاجهادات المحلية فى هذه العينات هى شد – ضغط و لكن فى عينات (صفر، ٩٠°) فأنها معرضة محليا لاجهادات قص فقط. عند نسب الاجهاد السالبة فان وجود اجهاد متوسط يسبب تاثير ضارا على قيمة الاجهاد المتغير فى عينات (± ٤٥°) فى الوقت الذى لم يكن له تاثير ملحوظ على عينات (صفر، ٩٠°) فى المنطقة الاولى ولكن فى المنطقة الثانية كان له تاثير ضار.وقد تم دراسة سلوك الكلال نظريا للعينات تحت نسب اجهاد موجبة وقد وجد انه بالنسبة للعينات (صفر، ± ٤٥°) فانه لايوجد علاقة تربط بين القيمة فى حالة نسب الاجهاد الموجبه ونظيرتها فى حالة النسب السالبة فى الوقت الذى وجد فى حالة عينات (صفر، ٩٠°) انه عند نفس العمر فان الاجهاد المتغير يتناقص مع ازدياد الاجهاد المتوسط.

Keywords: Glass fiber, Reinforced polyester, Torsional fatigue, Mean stress, Stress ratio

1. Introduction

It is well known that, the compressive mean stress has no effect on the fatigue behaviour of different metals, which may be beneficial; while the tensile mean stress always tends to decrease their fatigue resistance. On the other hand, it was found that, up to a certain limit the torsional mean stress has no effect on the torsional endurance limit of metals [1]. Wöhler demonstrated that the stress range necessary to produce fracture in metals subjected to normal stress decreases as the mean stress increases [2]. As a consequence of the work of Wöhler and others, various relationships have been proposed to account for the effect of mean stress, and in the most general form, all these relationships may be represented mathematically by the following equation:

$$\sigma_a = \frac{S_e}{f.o.s}\left(1-\left(\frac{\sigma_m}{S / f.o.s}\right)^n\right),$$

Where:
S_e is the endurance limit,
S is the limiting static strength,
n is the material constant,
$f.o.s$ is the factor of safety, and
σ_m and σ_a are the mean and amplitude normal stress components, respectively.

El-Kadi and Ellyin [3] studied the effect of stress ratio (*R*), which represents the ratio between the minimum and maximum stresses, on the fatigue behaviour of unidirectional laminae. They used glass-epoxy specimens subjected to off-axis tensile loading with different stress ratios. The results showed that for off-axis loading cases, the slope of the S - log (N) line for R = 0.5 is considerably smaller than that of R = 0. In other words, when the stress ratio (R) increases the rate of fatigue strength degradation decreases.

Bradley [4] studied the fatigue behaviour of unidirectional SiC/Ti-15-3 composite under both tension and compression with different mean stresses. He found that the tensile mean stresses were detrimental and that compressive mean stresses were beneficial to the fatigue strength, which was similar to their effects on the fatigue behaviour of metals. Several mean stress models (Smith-Watson-Topper, Walker, Normalized Goodman and Soderberg models) were examined for applicability to this class of composite materials, and the Soderberg approach was shown to best represent the effect of mean stress over the covered range. The other models varied significantly in their predictability and often failed to predict the composite behaviour at very high tensile mean stresses.

Rotem [5] studied the fatigue behaviour of graphite/epoxy composite laminates under tension-tension; compression-compression and tension-compression loading with different stress ratios. Using flat specimens with V_f ≈ 62.4 %. An envelope was drawn for each number of cycles to failure. The envelope indicated the specific failure mode for any stress ratio and number of cycles. He also found out that, the identification of the failure mode when the mean stress is not zero is not so simple, that is because; when the material starts to disintegrate close to final failure the mean load pushes the specimen in its direction regardless of the fracture mode. As a result, tensile failure mode with fibre fractures and cracks along the fibres may appear as compressive failure mode as a result of the final compression of broken specimen parts caused by the compressive mean load. Moreover, unlike conventional materials, sometimes by increasing mean stress the fatigue life becomes longer.

Sharara [6] studied the effect of stress ratio on the fatigue characteristics of GFRP subjected to bending moments. He used thin-walled tubes made from two layers of woven–roving E-glass/polyester with two fibre orientations, $[\pm 45^o]_{2s}$ and $[0,90^o]_{2s}$, with a fibre volume fraction (V_f) ranging from 50% to 64%. The mean stress component was found to have a detrimental effect on the amplitude stress component for both fibre orientations under negative stress ratios (R=-1, -0.75,-0.5,-0.25, 0).

1.1. The Smith-Watson-Topper (SWT) parameter

For metals, it was found that, plotting the fatigue life against the SWT parameter, which represents the square root of the maximum stress and amplitude stress components, when having normal stresses with different mean values, tends to plot a single curve. Consequently, it was possible to characterize the complete mean stress effect for a given metal with only a single stress ratio, for example: R = -1 [7].

The SWT parameter ($\sqrt{\tau_{max}\tau_a}$) was found to be valid for woven-roving GFRP under torsional moments by Nasr [8]. Thin-walled tubes with $[\pm 45^o]$ and $[0,90^o]$ fibre orientations were tested under negative stress ratios, and the SWT parameter tended to plot a single curve when plotted versus the number of cycles to failure. Besides, the SWT parameter was found to be valid for similar specimens subjected to bending moments with the same stress ratios.

Using the power formula: SWT = $c\,N^d$ has resulted in having a nearly constant ratio between (c) and the corresponding static strength for both fibre orientations, being nearly equal to unity.

In this work, the effect of torsional mean stresses on the fatigue behaviour of Glass Fiber-Reinforced Polyester (GFRP) is studied via testing thin-walled, woven-roving specimens with two fibre orientations, $[\pm 45^o]$ and $[0,90^o]$, at negative stress ratios (R), R = 1, -0.75, -0.5, -0.25, 0.

2. Experimental work

Most researchers use the stress ratio (R) when dealing with the effect of mean stress under different loading conditions [7-12]. The stress ratio (*R*) is defined to be the ratio between the minimum and maximum applied stresses. Consequently, torsional fatigue tests were performed on thin-walled tubular specimens at different negative stress ratios, R = -1, -0.75, -0.5, -0.25, 0.

2.1. Testing machine

The used testing machine was previously designed by Abouelwafa et al. [13] and used by other researchers in similar works [5,7, 14, 15]. It is a strain controlled testing machine, rotating at a constant speed of 525 rpm (8.75 Hz); and capable of performing pure torsion, pure bending, or combined torsion and bending (in-phase or out-of-phase) fatigue tests. Fig. 1 shows a general layout for the machine, the loading systems (torsion and bending) are independent, and have the facility to apply different mean stresses. The specimen is subjected to a uniform load, along its whole length, through a gripping system consisting of two halves that enclose the specimen in between. The applied torque was measured via a load cell, fixed on one of the grippers, consisting of four active strain gauges, forming a full bridge. The signal is amplified and displayed on an oscilloscope and the whole system was calibrated.

2.2. Specimens

Thin-walled tubes made from two layers of woven-roving E-glass/polyester with two fibre orientations, $[\pm 45^o]_{2s}$ and $[0,90^o]_{2s}$ were used with a fibre volume fraction (V_f) ranging from 55 % to 65 %. This range was used in previous works [2,14, 15,] and has proved its suitability to ensure good adhesion between fibres and matrix, good strength and acceptable mechanical properties. Table 1 shows the properties of the used materials. Cobalt Naphthenate (6 % solution) was used as an accelerator in a percentage of 0.2 %, by volume, and Methyl Ethyl Ketone (MEK) peroxide as a catalyst in a percentage of 2 %, by volume [7, 14, 15, 16, 17]. Cross-linking and curing took place at ambient conditions. Fig. 2 shows the nominal dimensions of the used specimens, with tolerance ± 0.1 mm, which where measured after complete curing and being within the standard dimensions [7, 14, 15]. The thickness of the tube ends were built up by additional two layers to avoid gripping problems, and to gradually introduce the load so that failure occurs in the central, uniformly stressed portion of the tube [18, 19].

2.3. Stress state

Specimens are subjected to torsional fatigue moments with different mean values. Being cylindrical in shape, their global stress (τ_{xy}) may be found from the following equation:

$$\tau_{xy} = \frac{Tr}{J},$$

where:

T	is the applied torque ($T = T_m + T_a \sin \omega t$),
T_m and T_a	are the mean and amplitude torques, respectively,
(ωt)	is the twisting angle, and
J	is the second polar moment of area.

$$J = \frac{\Pi}{32}\left(d_o^4 - d_i^4\right),$$

(d_o) and (d_i) are the outer and inner diameters of the specimen, respectively and $r = d_o / 2$. The $[\pm 45^o]_{2s}$ specimens had a tension - compression local stress state, $\sigma_1 = -\sigma_2 = \tau_{xy}$ and $\sigma_6 = 0$, while the $[0,90^o]_{2s}$ specimens had a pure local shear stress state, $\sigma_1 = \sigma_2 = 0$ and $\sigma_6 = \tau_{xy}$.

3. Test results

It is important to note that, in order to avoid any misleading data, only the specimens that had their failure features within the accepted gauge section, the middle third of the whole length were considered; while those that have their failure due to any gripping problems were excluded. Each experimental data point was obtained by considering the average of three specimens tested under the same conditions

3.1. Static tests

Static torsional tests were performed on the tubular specimens of both orientations, [± 45°]$_{2s}$ and [0,90°]$_{2s}$, in order to find out their ultimate global shear strengths (S_{us}), which was found to be as follows;

- (S_{us}) of the [0,90°]$_{2s}$ pecimens = 47 MPa

- (S_{us}) of the [± 45°]$_{2s}$ specimens = 76 MPa

3.2. Fatigue tests

All specimens were tested under ambient conditions and constant frequency of 8.75 Hz. The data points were used to plot the corresponding *S-N* curves on a semi-log scale, being fitted using the power law: maximum stress = aN^b, representing the torsional fatigue shear strength (S_{fs}). Failure was considered to occur when the load reading decreased by about 20% of its original value. In other words, 20 % reduction in the strength of the specimen will represent failure. Tests were performed on both fibre orientations, [± 45°]$_{2s}$ and [0,90°]$_{2s}$, at five different stress ratios (R = -1, -0.75, -0.5, -0.25, 0). Figs. 3 and 4 show the corresponding *S-N* curves at all stress ratios for both fibre orientations. The two constants (a) and (b) were found to have the values given in table 2. The fatigue ratio, the ratio between the fatigue endurance limit (S_{es}) to the corresponding static failure strength (S_{us}), was found to be 0.23.

4. Analysis and discussion

4.1. Analysis of the S-N curves

Using the power formula: $\tau_{max} = aN^b$ has proved its suitability by giving acceptable values for the correlation factor, table 2. Analyzing the values of the two constants (a) and (b), resulted in the following conclusions:
1. The deviation in the values of (a) at different stress ratios is negligible and it may be considered to be constant, considering each of [± 45°]$_{2s}$ and [0,90°]$_{2s}$ specimens separately. The average value of (a) was calculated and considered to be used at any stress ratio, as the corresponding standard deviation was found to have acceptable values, as shown in table 3.

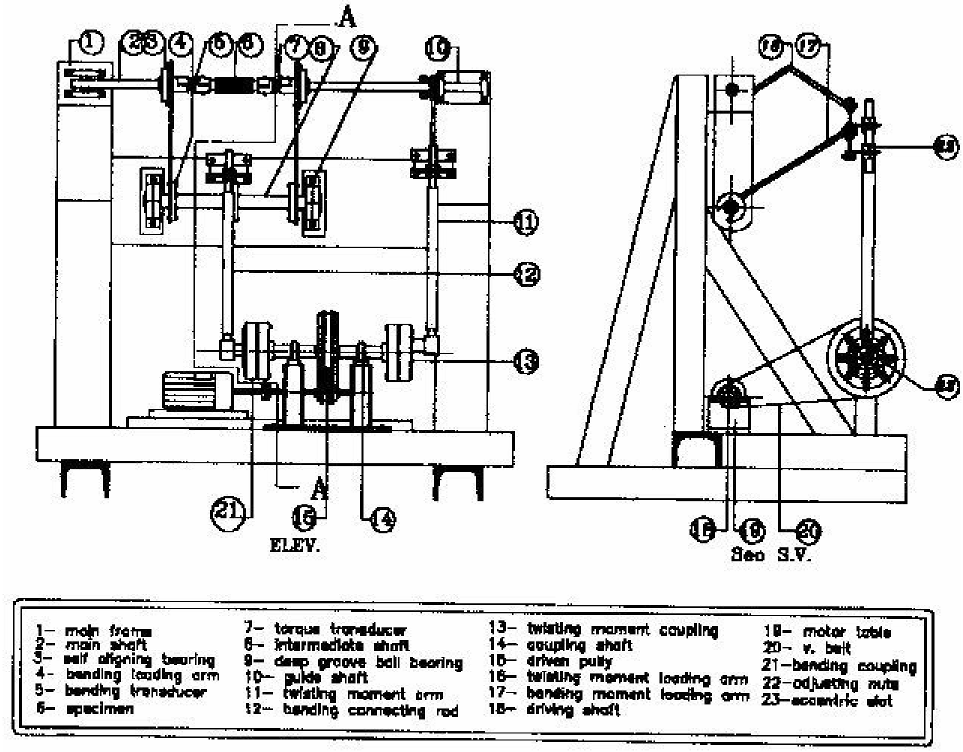

Fig. 1. General layout of the testing machine.

Table 1
Properties of used materials [15, 20, 21]

Woven–roving E-glass fibres		Polyester	
Property	Value	Property	Value
Density	2551 kg / m^3	Density	1161.3 kg / m^3 (Measured)
Modulus of elasticity	E = 76 GPa	Modulus of elasticity	E = 3.5 GPa
Poisson's ratio	υ = 0.37	Poisson's ratio	υ = 0.25
Tensile strength	3.45 GPa	Gel time at 25 °C	20 min.
Average mass / area	600 gm / m^2	Viscosity	0.45 Pa.s
Average thickness	0.69 mm	Percentage of styrene	40 %
Weave	Plain	Trade name	Siropol 8340

Table 2
Fatigue constants (a) and (b) for both fibre orientations

	[± 45°]$_{2s}$ Specimens			[0,90°]$_{2s}$ Specimens		
Stress ratio (R)	a (MPa)	b	Correlation factor	a (MPa)	b	Correlation factor
-1	103.885	-0.130215	0.98944	60.9202	-0.120095	0.95403
-0.75	102.809	-0.124325	0.9891	60.5911	-0.109763	0.99457
-0.5	103.684	-0.114509	0.98867	60.1193	-0.096862	0.98431
-0.25	103.712	-0.104432	0.97557	59.915	-0.089564	0.94718
0	103.685	-0.094781	0.9926	59.4429	-0.071927	0.93806

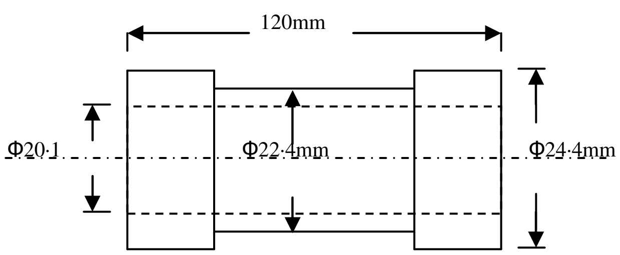

Fig. 2. Dimensions of used specimens.

Table 3
Average values of (a) for the tested specimens, $\tau_{max} = a\,N^{-b}$

Specimen type	Average value of (a): (MPa)	Standard deviation (%)
[± 45°]$_{2s}$	103.555	0.4
[0,90°]$_{2s}$	60.1968	0.96

2. One can notice that the average (a) value of the [± 45°]$_{2s}$ specimens is higher than that of the [0,90°]$_{2s}$ specimens, with nearly the same ratio of their static torsional strengths.

$(a)_{[\pm 45]} / (a)_{[0,90]} = 1.72$ and,

$(S_{us})_{[\pm 45]} / (S_{us})_{[0,90]} = 1.62$

This leads us to an important conclusion; that the value of (a) is constant and function of the static strength of the tested material. Finding the value of (a) as a ratio of (S_{us}) we found that:

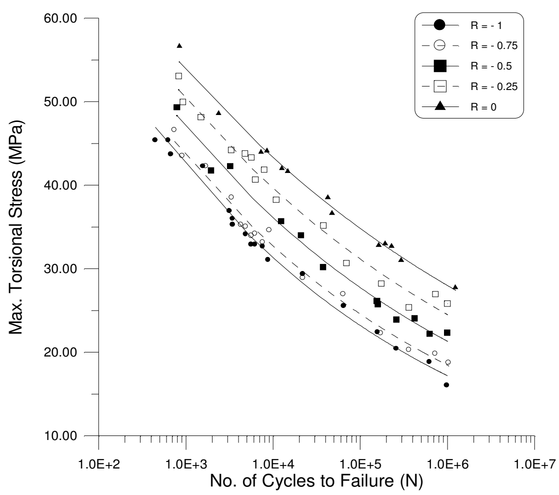

Fig. 3. Torsional S-N curves of [± 45°]$_{2s}$ specimens.

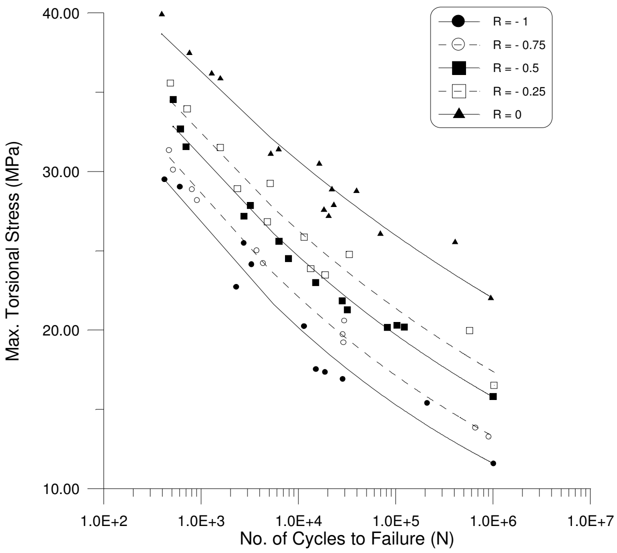

Fig. 4. Torsional *S-N* curves of $[0,90^o]_{2s}$ specimens.

$(a\ /\ S_{us})_{[\pm 45]} = 1.363$ and $(a\ /\ S_{us})_{[0,90]} = 1.281$.

3. The value of the power (b) was found to depend on the stress ratio (R) for both fibre orientations, and the fitted relations were as follows:

$(b)_{[\pm 45]} = 0.0363044\ R - 0.0955002$
$(b)_{[0,90]} = 0.0467334\ R - 0.0743361$

Increasing the value of (R) causes a decrease in the corresponding absolute value of (b); i.e. the fatigue strength degradation rate decreases with the increase of (R).

4. Comparing the values of the power (b) of the $[\pm 45^o]_{2s}$ to the $[0,90^o]_{2s}$ specimens shows that: at all the tested stress ratios, the $[\pm 45^o]_{2s}$ specimens always have higher powers; i.e. they have higher failure rates. This may be explained in terms of the different local stresses found in both specimens; the tension component found in the $[\pm 45^o]_{2s}$ specimens causes fibre failures (brittle failure), while the $[0,90^o]_{2s}$ specimens were subjected to pure shear, resulting in gradual strength degradation. Talreja. [22] did found the same results, but for different conditions.

5. Considering the local stress state, since the $[\pm 45^o]_{2s}$ specimens are subjected to tension - compression while the $[0,90^o]_{2s}$ specimens are subjected to pure shear, it was found that the $[\pm 45^o]_{2s}$ specimens have higher torsional strength than the $[0,90^o]_{2s}$ specimens at all stress ratios. This was also found in many other researches [2, 6, 22, 23, 24]. Besides, the *S-N* curves of both orientations do not intersect at any stress ratio; i.e. although the $[\pm 45^o]_{2s}$ specimens have higher failure rates but they are still stronger than the $[0,90^o]_{2s}$ specimens at all stress ratios and at any life, this is because of the great difference in their static torsional strength.

According to the first and third conclusions, the average governing *S-N* equations are:

$$\tau_{max} = 103.555\ N^{(0.0363044\ R - 0.0955002)}$$
for $[\pm 45^o]_{2s}$ specimens, (1-a)

$$\tau_{max} = 60.1968\ N^{(0.0467334\ R - 0.0743361)}$$
for $[0,90^o]_{2s}$ specimens. (1-b)

4.2. Expected positive stress ratio points

Using eq. (1), the *S-N* equations for the positive stress ratios were found by extrapolation. These extrapolated equations, table 4, only represent expected values, while it is recommended to check the fatigue behaviour under positive stress ratios experimentally.

4.3. Mean-amplitude diagrams

The mean-amplitude diagrams were plotted at different lives for each of the $[\pm 45^o]_{2s}$ and $[0,90^o]_{2s}$ specimens, as shown in fig. 5 and fig. 6. The need for groups of specimens, one at each stress ratio, having exactly the same life; make it impossible to use the actual experimental data in plotting the mean-amplitude relations. On the other hand, we used the fitted *S-N* equations to find out the required points; using these fitted equations is supported by having high correlation factors.

Table 4
S-N equations of the expected positive stress ratio

Stress ratio (R)	$[\pm 45^o]_{2s}$ specimens	$[0,90^o]_{2s}$ Specimens
0.25	$103.555\ N^{-0.086424}$	$60.1968\ N^{-0.0626527}$
0.5	$103.555\ N^{-0.077348}$	$60.1968\ N^{-0.0509694}$
0.75	$103.555\ N^{-0.0682719}$	$60.1968\ N^{-0.039286}$

Plotting the mean-amplitude components of the $[\pm 45^o]_{2s}$ specimens representing the negative stress ratios and using the static point (S_{us}, 0) gave straight line relations, as shown in fig. 5, with high correlation factors. This supports the use of an equation in the same form as Goodman's equation for normal stresses to be the governing equation for the mean-amplitude relation.

Therefore, the equation: $\frac{\tau_m}{S_{us}} + \frac{\tau_a}{S_{fs}} = 1$ is suitable for representing the effect of the mean stress in the $[\pm 45^o]_{2s}$ specimens. In other words, when the composite has a stress state of: $\{\sigma_1 = -\sigma_2$ and $\sigma_6 = 0\}$, it behaves similar to metals subjected to normal stresses. Consequently, the equivalent static stress ($\tau_{eq.}$) will take the form shown in eq. (2).

$$(\tau_{eq.})_{[\pm 45^o]} = \tau_m + \left(\frac{\tau_a}{S_{fs}}\right) S_{us} \,. \qquad (2)$$

When we tried to include the points representing the positive stress ratios in drawing the mean-amplitude relations; we found that these points are not suitable to be used in this manner, lowering down the correlation factors and violating eq. (2). This was expected because it is known that the behaviour of composites differs greatly when subjected to tension-tension, tension-compression, or compression-compression [25, 15, 5, 26, 27, 28].

When plotting the mean-amplitude components of the $[0,90^o]_{2s}$ specimens, they showed an apparent difference from those of the $[\pm 45^o]_{2s}$ specimen as shown in fig. 7. At low stress levels, all the points tend to fit a horizontal straight line representing their average value, region (1); which was found to be 0.982 of the fatigue shear endurance limit (S_{es}) at $N = 10^6$ cycles with an acceptable standard deviation (3.725 %). In other words, the mean stress seems to be ineffective, and the amplitude stress may be considered equal to the corresponding fatigue strength (S_{fs}). But, the range for which the mean stress is ineffective decreases when the number of cycles to failure decreases, or when the maximum stress increases; i.e. the horizontal straight line succeeds in fitting some of the points and not all of them when the number of cycles to failure decreases, but it still represents the corresponding fatigue strength (S_{fs}).

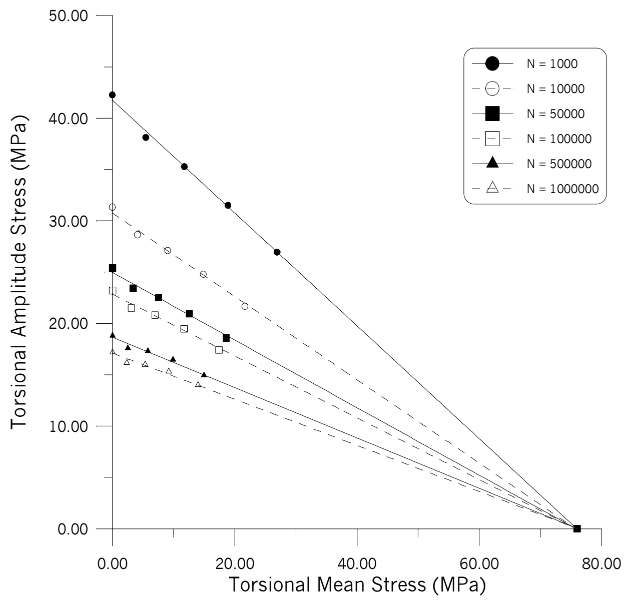

Fig. 5. Mean-amplitude relation for the $[\pm 45^o]_{2s}$ specimens.

Consequently, the mean stress component was found to be ineffective up to certain stress ratios according to the applied maximum stress. For number of cycles to failure ranging from $4*10^5$ to 10^6 cycles the mean stress was found to be ineffective for the region between R = -1 and R = 0, region 1 in fig. 7 as an example, and the range of this region decreases when the number of cycles to failure decrease, table 5. This arises in a similar behaviour to that of metals subjected to shear stresses, which may be explained in terms of the local stress state of the $[0, 90^o]_{2s}$ specimens. These specimens were subjected to a pure shear stress, that results in matrix dominated failure modes, and since the fatigue process in polymers is similar to that in metals [3], then it is logically to find the $[0, 90^o]_{2s}$ specimens behaving like metals in this case. The points representing the positive stress ratios were omitted in the case of the $[\pm 45^o]_{2s}$ specimens, as they were not compatible with the experimental negative stress ratio points. But, here for the $[0,90^o]_{2s}$ specimens, these points had shown a totally new behaviour with respect to the original negative stress ratios, which worth to be studied and checked out. They plotted a straight line starting from the end of region 1 fig. 6, and ending by the static point (S_{us}, 0) with good correlation factors in the whole range, constructing region 2 in fig. 6. It was found that, the slope of the inclined straight line increases with the decrease of the number of cycles to failure.

Since the $[0,90^o]_{2s}$ specimens have a pure local shear stress state, without any tension or compression components, thus; one may expect no the agreement between positive and negative stress ratio points in this case. The inclined straight line of region 2. Fig. 6 showed acceptable correlation factor with the used points; resulting in very good correlation factors being 0.9887.

The straight-line equation was found to be dependent on the range of the corresponding fatigue life, and the general formula is given by eq. (3):

$$\frac{\tau_m}{S_{us}} + K_{mn}\frac{\tau_a}{S_{fs}} = 1 \,. \qquad (3)$$

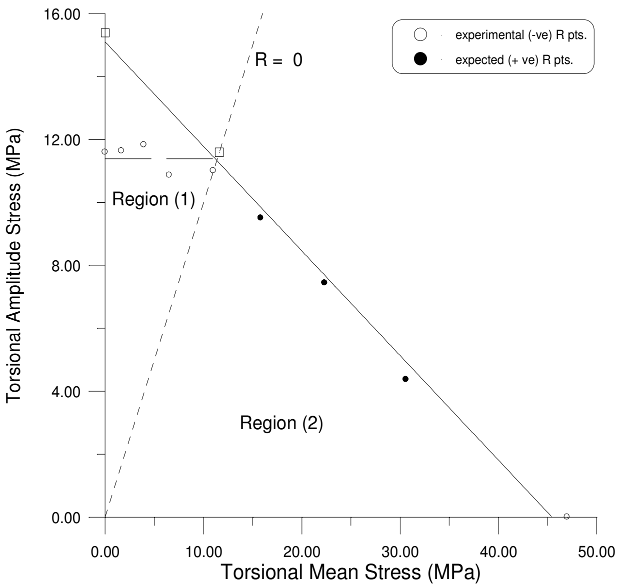

Fig. 6. Mean-amplitude relation for the $[0,90^o]_{2s}$ specimens at 10^6 cycles.

Table 5
Different values of R_m

Range of failure life (cycles)	R_m
From $5*10^3$ to $9*10^4$	- 0.5
From 10^5 to $3*10^5$	- 0.25
From $4*10^5$ to 10^6	0

where,

$$K_{mn} = \frac{S_{us} - C_{mn}\, S_{fs}}{S_{us}} \quad \text{and} \quad C_{mn} = \frac{1+R_m}{1-R_m}\,,$$

R_m represents the stress ratio separating the two regions 1 and 2. The values of R_m with the corresponding range of lives are shown in table 5.

The constant (K_{mn}) was referred to as; "equivalent static shear stress modifying constant" and the equivalent static shear stress ($\tau_{eq.}$) will be calculated from eq. (4).

$$\left(\tau_{eq.}\right)_{[0,90^o]} = \tau_m + K_{mn}\left(\frac{\tau_a}{S_{fs}}\right) S_{us} \qquad (4)$$

Although the proposed procedure has proved its suitability to the studied case, with high correlation factors, we suggest checking the behaviour of these specimens under positive stress ratios experimentally.

5. Conclusions

1. Using the power formula: $\tau_{max} = aN^b$ has proved its suitability for $[\pm 45^o]_{2s}$ and $[0,90^o]_{2s}$ specimens subjected to torsional fatigue loading with different mean values. The two constants (a) and (b) were found to follow the following behaviour:

- The value of (a) was found to have a constant value for each fibre orientation, representing a certain ratio from the corresponding static strength. This ratio seems to be nearly constant for both orientations with a slight deviation and being around 1.28, for conservative results. In other words, the value of (a) depends only on the static strength of the material and not the stress ratio (R).
- The value of the power (b), which represents the failure rate, was found to depend on both the static strength of the material and the stress ratio (R). The $[\pm 45^o]_{2s}$ specimens had higher failure rates that was attributed to the brittle fibre failure due to the tension stress component.

2. The mean stress component is ineffective for specimens under pure local shear stress,

[0,90°] fibre orientation, to a certain stress ratio, region 1. Fig. 6, this region decreases when the number of cycles to failure decreases. In other words, the effectiveness of the mean stress component increases when moving towards static loading, table 5. After this region the mean stress component is found to have a detrimental effect on the amplitude component for the same life, region 2 in fig. 6, and being governed by the following equation:

$$\frac{\tau_m}{S_{us}} + K_{mn}\frac{\tau_a}{S_{fs}} = 1 \ .$$

The constant (K_{mn}) was referred to as the "equivalent static shear stress modifying constant", and is given by the following equation:

$$K_{mn} = \frac{S_{us} - C_{mn}\, S_{fs}}{S_{us}} \quad \text{and} \quad C_{mn} = \frac{1 + R_m}{1 - R_m}$$

The value of R_m was found to vary with the specimen's life, table 5. It worth mentioning that, region 2 still requires experimental support.

3. When specimens were subjected to tension -compression local stress components, [±45°] fibre orientation, the mean stress was found to have a detrimental effect at all negative stress ratios. The classical Goodman's equation for normal stresses replaced by the corresponding shear stresses was found to govern the fatigue behaviour of the woven-roving GFRP, as follows:

$$\frac{\tau_m}{S_{us}} + \frac{\tau_a}{S_{fs}} = 1.$$

References

[1] J.E. Shigley, Mechanical Engineering Design, McGraw-Hill, (ISBN: 0-07-056898-7) (1986).

[2] A.A. El-Midany, Fatigue of Woven-Roving Glass Fibre Reinforced Polyester Under Combined Bending and Torsion, PhD. Thesis, Alexandria University-Egypt (1995).

[3] El Kadi, and F. Ellyin, "Effect of Stress Ratio on the Fatigue of Unidirectional Fibreglass-Epoxy Composite Laminae", J. of Composite Material (1993).

[4] L. Bradely "Model Determined for Predicting Fatigue Lives of Metal Matrix Composites Under Mean Stresses", www.grc.nasa.gov.

[5] Rotem, "Tensile and Compressive Failure Modes of Laminated Composites Loaded by Fatigue with Different Mean Stress", J. of Composites Technology & Research, Vol. 12, pp. 201- 208 (1990).

[6] A.I. Sharara, Effect of Stress Ratio on Fatigue Characteristics of Woven-Roving Glass Reinforced Polyester", MSc. Thesis, Alexandria University - Egypt (1997).

[7] Conle, and J.P Ingall, "Effects of Mean Stress on the Fatigue of Composite Materials", J. of Composites Technology &Research, Vol. 7, pp. 3-11 (1985).

[8] M. Nasr, the Effect of Mean Stress on the Fatigue Behaviour of Woven-Roving GFRP Subjected to Torsional Moments, MSc. Thesis, Alexandria-Egypt (2002).

[9] M.J. Robert, Mechanics of Composite Materials, McGraw-Hill Kogakusha, Ltd., (ISBN: 0-07-032790-4) (1975)

[10] W.T. Stephan, and M.W. Edward, "A General Theory of Strength of Anisotropic Materials", J. of Composite Materials, Vol. 5, pp. 58-80 (1971).

[11] E. Krempl, D.M. Elzey, B.Z. Hong, T. Ayar, and R.G Loewy, "Uniaxial and Biaxial Fatigue Properties of Thin-Walled Composite Tubes", J. of The American Helicopter Society, pp. 3-10 (1988).

[12] R. Talreja, “Fatigue of Composite Materials: Damage Mechanisms and Fatigue Life Diagrams”, Proc. of the Royal Society, Series A, Vol. 378 (1981).

[13] S. Satish, "Analysis of Local Delaminations Caused by Angle Ply matrix Cracks", J. of Composite Materials, Vol. 30 (4), pp. 418-453 (1996).

[14] M.R. Bhat, M.A. Majeed, and C.R.L. Murthy, "Characterization of Fatigue Damage in Unidirectional GFRP Composites through Acoustic Emission Signal Analysis", NDT and E

International, Vol. 27 (1), pp. 27-32 (1994).
[15] K.L. Reifsnider, Fatigue of Composite Materials, Elsevier Science Publishers, (ISBN: 0-444-70507-4) (1991).
[16] C.C. Christos, "Mechanics of Load Transfer at the Fibre / Matrix Interface", NASA Technical Note, NASA TN D-6588, (1972).
[17] P.S. James, The Science and Design of Engineering Materials, McGraw-Hill, (ISBN:0-256-24766-8) (1999).
[18] Z. Hashin, and A. Rotem, "A Fatigue Criterion for Fibre Reinforced Materials", J. of Composite Materials, Vol. 7, pp. 448 - 464 (1973).
[19] J.J. Nevadunsky, and J.J. Lucas, "Early fatigue Damage Detection in Composite Materials", J. of Composite Materials, Vol. 9, pp. 394-407 (1975).
[20] W.W. Stinchcomb, K.L. Reifsnider, L.A. Marcus, and R.S. Williams, "Effects of Frequency on the Mechanical Response of Two Composite Materials to Fatigue Loads", ASTM, STP 569, pp. 115 -129 (1975).
[21] C.K. Dharan, "Fatigue Failure Mechanisms in a Unidirectional Reinforced Composite Material", ASTM, STP 569, pp. 171-188 (1975).
[22] T. Ramesh, Fatigue of Composite Materials, Technomic Publishing Co., Inc., (ISBN: 87762-516 - 6) (1987).
[23] M.Y. Mohamed, the Inclusion Effect on the Fatigue Behaviour of Woven-Roving GRP Composite Materials, MSc.Thesis, Alexandria University - Egypt (2001).
[24] S.S. Wang, E.S.M. Chim, D.F. Socie, J.V. Gauchel, and J.L. Olinger, "Tensile and Torsional Fatigue of Fibre-reinforced Composites at Cryogenic Temperatures", J. of Engineering Materials and Technology, Vol. 104, pp. 121-127 (1982).
[25] M.W. Hyer, Stress Analysis of Fibre-Reinforced Composite Materials, McGraw - Hill, (ISBN: 0 - 07-016700 -1) (1998).
[26] Mahfouz, "Response of Resin Transfer Moulded (RTM) Composites Under Reversed Cyclic Loading", J. of Engineering Materials & Technology, Vol. 118, pp. 49-57 (1996).
[27] Z. Hashin, "Fatigue Failure Criteria for Unidirectional Fibre Composites", J. of Applied Mechanics, Vol. 48, pp. 846-852 (1981).
[28] M.J. Owen, and J.R. Griffiths, "Evaluation of Biaxial Stress Failure for a GFRP Under Static and Fatigue Loading", J. of Material Science, Vol. 13, pp. 1521-1537 (1978).

Received June 17, 2004
Accepted January 6, 2005